

## The Kinetics of Carbon Formation From $\text{CH}_4 + \text{H}_2$ on a Silica-Supported Nickel Catalyst

I. ALSTRUP\* AND M. TERESA TAVARES†

\*Haldor Topsøe Research Laboratories, DK-2800 Lyngby, Denmark;  
and †Centro de Química Pura e Aplicada (INIC), Universidade do Minho,  
4719 Braga Codex, Portugal

Received June 21, 1991; revised November 15, 1991

A microkinetic model for the formation of carbon on a nickel surface exposed to  $\text{CH}_4 + \text{H}_2$  gas mixtures is constructed and compared with measured carbon formation rates for a Ni/SiO<sub>2</sub> catalyst. Most of the parameters of the model are determined independently from single-crystal experiments or from *ab initio* calculations. Two rate constants and two chemisorption bond energies are determined by least-squares minimization. Good agreement is obtained with the experimental values. The resulting values for the bond energies are in good agreement with values obtained by experiments and *ab initio* calculation. The bond energies as well as the ratio of the rate constants depend only weakly on the assumed carbon coverage. © 1992 Academic Press, Inc.

### 1. INTRODUCTION

The formation of various forms of carbonaceous solids on metals by the decomposition of carbon-containing gases has been studied for many years mainly because of its importance in catalysis and corrosion. New promising applications such as the production of high-quality carbon fibers and of diamond or diamond-like thin film coatings have recently added to this interest.

The increasingly utilization of natural gas, consisting mainly of methane, as an important raw material for the chemical industry has added strongly to the motivation of studies of the interaction of methane with various surfaces.

Recently a deeper understanding of the interaction of methane molecules with nickel surfaces has begun to emerge from experimental studies of the interaction of methane with single-crystal surfaces (1-3).

The chemisorption of methane on nickel surfaces is observed to have a very low probability and a high activation energy. By molecular beam studies (1) it was recently shown that the chemisorption on Ni(111) is dissociative resulting at low surface temper-

atures in stable  $\text{CH}_3$  surface species, which dehydrogenate stepwise on the surface at higher temperatures.

Long ago Grabke (4) demonstrated that kinetic measurements of carbon deposition on  $\alpha$ - and  $\gamma$ -iron surfaces exposed to  $\text{CH}_4 + \text{H}_2$  gas mixtures could be explained quantitatively by assuming a mechanism based on stepwise dehydrogenation of surface species after chemisorption of the methane molecule and with the dehydrogenation of methyl as the rate-limiting step. Grabke also showed that the same kinetic model could account for measurements on iron-nickel alloys with 10 and 20 wt% nickel. Lázár *et al.* (5) found that the deposition of carbon on nickel foils does not obey the Grabke model at low carbon activities. They also reported that Grabke found the rate of hydrogasification to be proportional to the hydrogen partial pressure. Figueiredo and Trimm (6) found the same hydrogen pressure dependence for the time-independent rate of hydrogasification of carbon on nickel foils and Ni/Al<sub>2</sub>O<sub>3</sub> catalysts. Moreover, they observed that in the case of nickel foils, the rate of hydrogasification was proportional to the amount of carbon initially present,

while no correlation was observed in the case of the supported catalyst. Audier and Coulon (7) found that the rate of carbon deposition on an iron–nickel catalyst with 75% nickel in both  $\text{CH}_4 + \text{H}_2$  and  $\text{CO} + \text{CO}_2$  mixtures depended solely on the carbon activity of the gas. Bernardo *et al.* (8) fitted a modified version of the Grabke kinetic expression to a small number of rates measured for carbon deposition from  $\text{CH}_4 + \text{H}_2$  mixtures on silica-supported Ni–Cu alloy catalysts. Baker *et al.* (9) and Rostrup-Nielsen and Trimm (10) on the other hand suggested that the diffusion of carbon through the nickel particle is the rate-limiting step during the steady-state growth of carbon filaments on Ni catalysts.

Recently we have studied the steady-state rates of carbon deposition on silica-supported nickel and nickel–copper alloy catalysts in  $\text{CH}_4 + \text{H}_2$  mixtures as a function of the partial pressures of  $\text{CH}_4$  and  $\text{H}_2$  (11). Various kinetic models have been tested on these data. It was shown (11) that the rates are not a simple function of the carbon activity but that models based on a modified Grabke kinetic model with dissociative chemisorption of methane can be fitted accurately to the experimental data if it is assumed that the carbon coverage is constant and that the other coverages are negligible. However, an equally good fit was obtained by assuming that either the chemisorption step or the first dehydrogenation step is rate limiting.

It has recently been shown for a few heterogeneous catalytic reactions that it is possible to construct a microkinetic model, which, with parameters determined from surface-science experiments, can account quantitatively for the observed rates (12). In the present case it has not yet been possible to carry out all the surface-science experiments necessary for the determination of the parameters of such a model. However, most of the parameters, which at present cannot be determined experimentally, have recently been calculated by an *ab initio* quantum chemical method. Based on these

results and available experimental single-crystal results a microkinetic model is constructed and discussed in the present work.

## 2. EXPERIMENTAL

The experimental conditions and the results have been reported in some detail in Ref. (11), so only a brief description is given here.

### 2.1. Catalyst Preparation

The Ni/SiO<sub>2</sub> catalyst with 20 wt% Ni was prepared by “dry” impregnation. The required amounts of nickel nitrate were dissolved in a volume of water equal to the measured pore volume of the support material (Cab-O-Sil H5). The solution and the support material were mixed and calcined at 773 K for 3 h. After addition of plasticizer and water, small pellets were extruded from the powder. The pellets were calcined for 2 h at 873 K. Finally the catalyst was pre-reduced at 773 K in H<sub>2</sub> for 44 h.

### 2.2. Characterization

Reduced catalyst samples were characterized by hydrogen chemisorption, X-ray diffraction, and nitrogen adsorption (11). The nickel area of the fresh catalyst calculated from the hydrogen chemisorption results was about 6 m<sup>2</sup>/g-cat, while the X-ray diffraction peak width corresponded to an average nickel particle size of about 20 nm in excellent agreement with results obtained previously for catalysts prepared in the same way (8).

### 2.3. Reactor System

The reactor system consisted of a microbalance (C.I. Electronics, MK2CT5) and associated flow reactor, furnace, flow, and temperature controllers. The rates of carbon deposition were determined from the slopes of the curves drawn by the microbalance recorder.

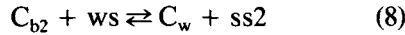
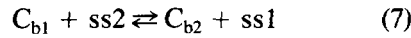
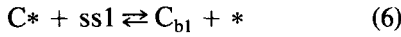
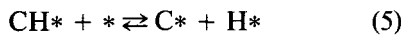
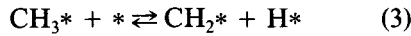
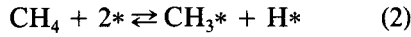
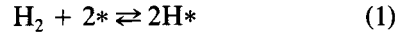
### 2.4. Experimental Conditions

Steady-state carbon deposition rates were measured at three temperatures (723, 773,

and 823 K), and at each temperature the partial pressures of methane and hydrogen were varied independently between 20 and 80 kPa and between 5 and 15 kPa, respectively. The steady-state rate was determined on a fresh catalyst sample at 24 different pairs of partial pressures at each temperature.

### 3. KINETIC MODEL

We use the model of Grabke (4) for carbon formation on iron as a starting point for the construction of a kinetic model for carbon formation on nickel. The molecular beam studies (1) of methane interacting with Ni(111) confirm the stepwise dehydrogenation of surface species but indicate that no precursor is involved in the dissociative chemisorption of the methane molecule. A direct dissociative chemisorption of methane is also in agreement with the results obtained by Chorkendorff *et al.* (3). Therefore we assume that the following steps govern the rates of carbon formation on the nickel catalyst:



where the asterisk (\*) signifies a surface site and CH<sub>x</sub>\* with  $x = 0, \dots, 3$  are chemisorbed species. C<sub>b1</sub> is a carbon atom in the bulk phase of the nickel crystal at a subsurface site ss1 just below the surface on which the surface reactions take place, and C<sub>b2</sub> is a carbon atom at a subsurface site ss2 just below the interface between the nickel particle and the carbon segregating out of the nickel particle. C<sub>w</sub> is a carbon atom at a site ws in the final carbon phase, which under

the present conditions is most probably a carbon filament (whisker) (8).

In order to be able to obtain a rate expression we make the following additional assumptions:

(i) All the steps are in quasi-equilibrium except one, which can be either step (2), the dissociative CH<sub>4</sub> chemisorption step, or one of the subsequent dehydrogenation steps, (3)–(5).

(ii) The surface species are all competing for the same surface sites and the occupation of a site is independent of the occupation of the other sites (Langmuir-type model).

The information necessary for a description of steps (6)–(8) is not available, but is not needed because of assumption (i), which means that these steps enter the rate expression through a constant carbon coverage only.

For each of the steps (2) to (5) assumed to be rate limiting we can derive a rate expression, which if step (2) is rate limiting turns out to be

$$r_2 = k_2(P_{\text{CH}_4}\theta_*^2 - \frac{1}{K_2}\theta_{\text{CH}_3}\theta_{\text{H}}) \quad (9)$$

with

$$\theta_{\text{CH}_3} = \frac{a_{\text{H}}^3}{K_3K_4K_5}\theta_{\text{C}}, \quad (10)$$

where

$$a_{\text{H}} = \sqrt{K_1P_{\text{H}_2}}$$

and if step (3) is rate limiting the expression

$$r_3 = k_3(\theta_{\text{CH}_3}\theta_* - \frac{1}{K_3}\theta_{\text{CH}_2}\theta_{\text{H}}) \quad (11)$$

is obtained with

$$\theta_{\text{CH}_3} = \frac{K_2}{a_{\text{H}}}P_{\text{CH}_4}\theta_*, \quad (12)$$

where  $K_n$ ,  $n = 1, \dots, 5$ , are equilibrium constants of steps (1) to (5) and  $k_2$  and  $k_3$  are rate constants of the forward rate of step (2) or (3), respectively.  $\theta_*$  is the concentration of unoccupied sites, i.e.,

$$\theta^* = 1 - \theta_H - \theta_{CH_3} - \theta_{CH_2} - \theta_{CH} - \theta_C, \quad (13)$$

where  $\theta_x$  is the concentration of sites occupied by species  $x$ .  $\theta_x$  is calculated from equilibrium expressions corresponding to steps (1), (5), and (4) for  $x = H$ ,  $x = CH$ , and  $x = CH_2$ , respectively:

$$\theta_H = a_H \theta^*, \quad \theta_{CH} = \frac{a_H}{K_5} \theta_C, \quad \theta_{CH_2} = \frac{a_H}{K_4} \theta_{CH}. \quad (14)$$

Expressions similar to Eqs. (9) and (11) are easily derived assuming one of the steps (4) or (5) to be rate limiting. A consequence of the assumption of quasi-equilibrium is, as mentioned above, that  $\theta_C$  stays almost constant irrespective of the hydrogen and methane pressures. If we assume that the coverages of the other surface species are negligible, the expressions (9) and (11) can be transformed into expressions linear in  $x$ , where

$$x = \frac{P_{CH_4}}{P_{H_2}^2}.$$

The dependent variables are

$$\frac{r_2}{P_{H_2}^2} \quad \text{and} \quad \frac{r_3}{P_{H_2}^{3/2}},$$

respectively.

It was shown in Ref. (11) that the experimental results at 723 K are in very good agreement with both of the two linear expressions based on the above assumptions and with step (2) or (3) as the rate-limiting step, respectively.

Similar plots corresponding to either step (4) or step (5) as rate limiting do not give a similar good agreement, so we conclude that it is highly probable that either step (2) or step (3) is rate limiting or that none of them can be considered to be close to equilibrium.

A more general model is derived by replacing assumption (i) with the assumption that neither step (2) nor step (3) is close to equilibrium and that rate  $r = r_2 = r_3$  (steady-state condition). This gives

$$\theta_{CH_3} = \frac{k_2 P_{CH_4} \theta^* + (k_3 \theta_C / K_3 K_4 K_5) a_H^3}{(k_2 / K_2) a_H + k_3}, \quad (15)$$

where

$$1 - \theta_C \left( 1 + \frac{a_H}{K_5} \left( 1 + \frac{a_H}{K_4} \left( 1 + \frac{k_3 a_H}{K_3 ((k_2 / K_2) a_H + k_3)} \right) \right) \right) \\ \theta^* = \frac{\left( 1 + \frac{k_3 a_H}{K_3 ((k_2 / K_2) a_H + k_3)} \right)}{1 + a_H + k_2 P_{CH_4} / ((k_2 / K_2) a_H + k_3)}, \quad (16)$$

which together with Eq. (14) allow us to calculate rates from Eqs. (9) or (11).

In the next section the equilibrium constants  $K_n$  of expressions (9), (11), (15), and (16) are calculated on the basis of available information about the properties of the gas molecules and the adsorbed species, and the resulting microscopic model is compared with the experimental data.

#### 4. MICROSCOPIC INTERPRETATION

The equilibrium constants of steps (1) to (5),  $K_1$  to  $K_5$ , can be calculated from the partition functions  $Z_x$ , where  $x$  is the formula for a molecule or a chemisorbed species:

$$K_1 = \frac{Z_H^{2*}}{Z_{H_2}} \quad (17)$$

$$K_2 = \frac{Z_{CH_3*} Z_{H*}}{Z_{CH_4}} \quad (18)$$

$$K_3 = \frac{Z_{CH_2*} Z_{H*}}{Z_{CH_3*}} \quad (19)$$

$$K_4 = \frac{Z_{CH*} Z_{H*}}{Z_{CH_2*}} \quad (20)$$

$$K_5 = \frac{Z_C^* Z_{H*}}{Z_{CH*}}. \quad (21)$$

The partition functions can be written as products of contributions from all the degrees of freedom

$$Z = Z_{\text{trans}} \prod_i Z_{\text{vib},i} \prod_j Z_{\text{rot},j} \exp(-E/k_B T). \quad (22)$$

The last term is the electronic contribution, which only contains the ground state energy. Electronic excitations can safely be neglected under the present conditions. The gas-phase data for the vibrational and rotational energies of H<sub>2</sub> and CH<sub>4</sub> are taken from Ref. (13). We use the convention that the enthalpy of formation of the elements is zero at 298.15 K, 1 atm.

The frequency of the vibration perpendicular to the nickel surface of adsorbed hydrogen atoms has been measured by Andersson (14). The bond energy of hydrogen atoms on clean nickel surfaces is known from experiments by Christmann (15).

The vibration frequencies of the intermediate surface species, CH<sub>3</sub>\*, CH<sub>2</sub>\*, and CH\* on Ni(111), have been measured by Lee *et al.* (1). It has not yet been possible to determine the chemisorption energies of these species, but recently Siegbahn and Wahlgren (16) have developed an ab initio method to the point where it can be expected to provide good estimates of these energies, i.e., with an accuracy of a few tens of kilojoules per mole. Very recently Siegbahn and Panas have published estimates of these energies (17).

The frequency of the vibration perpendicular to the nickel surface of adsorbed carbon atoms has been measured by Lehwald (18). Binding energies of carbon atoms on nickel surfaces have been inferred from carbon segregation studies by Isett and Blakely (19) and from studies of the equilibrium of the Boudouard reaction on a Ni/Al<sub>2</sub>O<sub>3</sub> catalyst by Takeuchi and Wise (20). Also a value for the C–Ni(100) bond energy has recently been estimated from ab initio calculations by Siegbahn and Panas (17).

## 5. RESULTS AND DISCUSSION

The only parameters of the model that cannot be taken from the literature are the rate constants  $k_2$  and  $k_3$ , the frequencies of vibration corresponding to the frustrated

translations of the chemisorbed species parallel to the surface, and the carbon coverage. The rate constant  $k_2$  has recently been measured accurately for Ni(100) (3), but the application of this result requires that we know the number of active nickel sites of the catalyst during the carbon deposition measurements.

We have estimated the frequencies corresponding to the frustrated translations of the chemisorbed species parallel to the surface by scaling one of the few measurements yet made of the frequency corresponding to a frustrated translation of a chemisorbed species parallel to the surface, viz. the frequency of the lateral vibrations of CO molecules chemisorbed on Ni(100) (21). The scaling is based on the assumption that the energy of the frustrated translation is proportional to  $(U/M)^{1/2}$  (cosine potential), where  $U$  is the potential well depth and  $M$  is the molecular mass and that  $U$  is proportional to the chemisorption bond energy.

The vibrational energies used in the model calculations are shown in Table 1 together with the theoretical values for the chemisorption bond energies. The bond energies for chemisorbed carbon atoms inferred from experiments are also shown.

Preliminary calculations showed that the accuracy of the fit of the model to the experimental data depends sensitively on the values used for the chemisorption energies of the carbon atom and hydrogen atom but only weakly on the properties of the other surface species. For  $\theta_c$  in the interval tested, 0.05 to 0.7, the accuracy of the fit does not depend on  $\theta_c$ .

Information about the carbon coverage under the steady-state reaction conditions is not available. However, if the reaction takes place mainly on Ni(100) surface facets, as recent studies indicate (22), then a lower limit to the carbon coverage can be inferred from the studies of Schouten *et al.* (23). They observed that at temperatures above about 600 K and above a minimum coverage, carbon atoms migrate into the bulk as driven by a constant source indepen-

TABLE 1  
Vibrational and Bond Energies of  
Chemisorbed Species

Species	Vibrational energies (J/mol)	Degeneracy	Chemisorption bond energy (kJ/mol)
H*	7240	1	264 <sup>a</sup>
	2000	2	
C*	4665	1	628 <sup>b</sup>
	1125	2	
CH*	35529	1	715, <sup>c</sup> 664–680 <sup>d</sup> 569 <sup>b</sup>
	15252	2	
	7776	1	
	749	2	
CH <sub>2</sub> *	31568	1	381 <sup>b</sup>
	32192	1	
	15579	1	
	9420	1	
	13641	1	
	13060	1	
	518	1	
	684	2	
CH <sub>3</sub> *	31761	1	193 <sup>b</sup>
	32658	2	
	14595	1	
	11544	2	
	15791	2	
	5802	1	
	4606	1	
607	2		

<sup>a</sup> Reference (15).

<sup>b</sup> Reference (17).

<sup>c</sup> Reference (19).

<sup>d</sup> Reference (20).

dent of the carbon coverage. At temperatures below about 1000 K part of the surface carbon is stable; thus at 723 K the migration cannot diminish the carbon coverage on Ni(100) below about 0.2 ML, where 1 ML =  $1.61 \times 10^{19}$  atoms/m<sup>2</sup>. A lower limit to  $\theta_c$  is thus 0.2 and as the rate of diffusion into the bulk is independent of the surface coverage it is consistent with the other assumptions of the model to assume that  $\theta_c = 0.2$ .

Consequently the bond energies of the chemisorbed carbon and hydrogen atoms together with the rate constants  $k_2$  and  $k_3$  have been used as parameters to be determined for  $\theta_c = 0.2$  by a nonlinear least-

squares minimization of the difference between model and experimental rates at 723 K.

The results obtained for  $k_2$ ,  $k_3$ ,  $E_{C^*}$ , and  $E_{H^*}$  for  $\theta_c = 0.2$  are shown in Table 2. The ranges of the calculated coverages of the intermediates and of hydrogen atoms are shown in Table 3. The results confirm that none of the steps can be considered close to equilibrium. The results also show that the coverages of the intermediates are very small while the hydrogen coverage is significant and comparable to the carbon coverage. The calculated and experimental rates are compared in Fig. 1. It is seen that the calculated and measured rates are in good agreement.

The accuracy of the determination of  $E_{C^*}$ ,  $E_{H^*}$ ,  $k_2$ , and  $k_3$  by the minimization procedure can be judged from the fact that a deviation from the minimum corresponding to variations of the experimental rates in accordance with the estimated accuracy is obtained by changes of  $E_{C^*}$ ,  $E_{H^*}$ ,  $k_2$ , and  $k_3$  of about 0.1, 0.2, 8, and 3%, respectively. To see what happens if  $\theta_c$  is larger than 0.2, the minimization has been carried out for a number of  $\theta_c$  values in the range 0.15 to 0.7. The results obtained for  $E_{C^*}$  and  $E_{H^*}$  are shown in Fig. 2 and for  $k_2$  and  $k_3$  in Fig. 3. It is seen that  $E_{C^*}$  and in particular  $E_{H^*}$  depend very weakly on the choice of  $\theta_c$ , while  $k_2$  and  $k_3$  increase strongly for higher carbon coverages. Even if it is assumed that  $\theta_c$  can have any value in the range 0.15–0.7 the model predicts the values of  $E_{C^*}$  and  $E_{H^*}$  quite accurately, i.e., in the ranges 676–692

TABLE 2  
Rate Constants for Steps 2 and 3 and Chemisorption  
Bond Energies for C\* and H\*

$\theta_c = 0.2$				
<i>T</i> (K)	$k_2$ (gC/gcat/atm/s)	$k_3$ (gC/gcat/s)	$E_{C^*}$ (kJ/mol)	$E_{H^*}$ (kJ/mol)
723	$3.15 \times 10^{-3}$	118	678	245
773	$5.33 \times 10^{-3}$	620	678	245
823	$8.45 \times 10^{-3}$	1400	678	245

TABLE 3

Coverage Ranges at 723 K for  $\theta_C = 0.2$ 

P <sub>CH<sub>4</sub></sub> = 0.2 – 0.9 atm, P <sub>H<sub>2</sub></sub> = 0.05 – 0.15 atm			
$\theta_H$	$\theta_{CH_3}$	$\theta_{CH_2}$	$\theta_{CH}$
0.12 – 0.19	$(1.2 - 5.1) \times 10^{-6}$	$(0.3 - 1.1) \times 10^{-5}$	$(1.2 - 2.1) \times 10^{-4}$

kJ/mol and 246–249 kJ/mol, respectively. The value for  $E_{C^*}$  is within the range of values inferred from the experiments of Takeuchi and Wise (20) of carbon formation on a Ni/Al<sub>2</sub>O<sub>3</sub> catalyst and also in agreement with the value calculated by Siegbahn and Panas (17). These authors suggest, however, that the relaxation of the nickel surface atoms is smaller in a real surface than in the cluster model used in the calculation, but the size of the correction is not known. The  $E_{H^*}$  value obtained is also reasonable taking the expected influence of surface carbon into account. Ko and Madix (24) found that the

presence of a carbon  $p(2 \times 2)$  structure ( $\theta_C \approx 0.4$ ) on Ni(100) diminished the hydrogen chemisorption energy by ca. 40 kJ/mol.

The rate constants  $k_2$  and  $k_3$  increase by almost an order of magnitude when  $\theta_C$  is increased from 0.15 to 0.7. However, the results indicate that the ratio  $k_3/k_2$  does not depend on  $\theta_C$ . The ratio values obtained from the minimizations are randomly distributed around a mean value of about 51000 with a standard deviation of 9100. With this result in mind it is to be expected that the temperature dependence of  $k_3$  can be determined by using  $\theta_C = 0.2$  also at 773 and 823

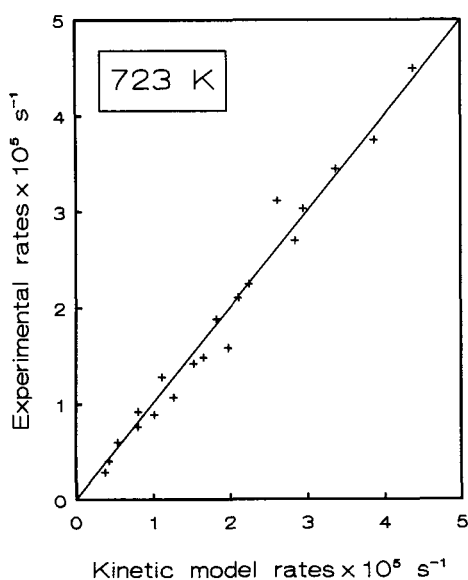


FIG. 1. Comparison between calculated and measured rates of carbon formation on Ni/SiO<sub>2</sub> at 723 K from CH<sub>4</sub> + H<sub>2</sub> gas mixtures. The rate unit is 10<sup>-5</sup> gcarbon/gcat/s.

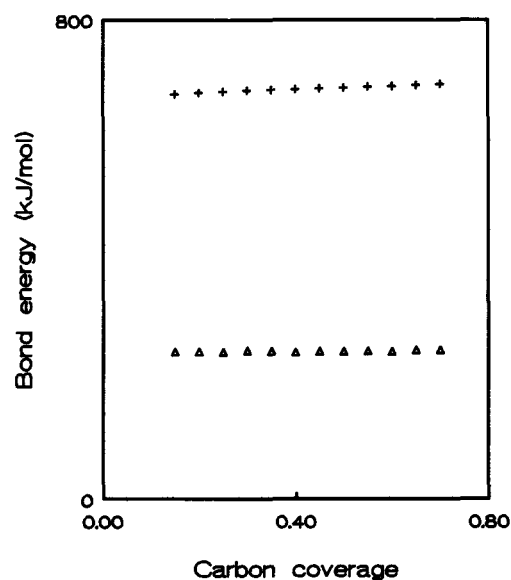


FIG. 2. Carbon coverage dependence of the chemisorption bond energies for carbon and hydrogen atoms on nickel for the optimized model. (+) carbon, (Δ) hydrogen.

K and adjusting the model parameters to obtain agreement with the experimental rates also at these higher temperatures.

The temperature dependence of the rate of the dissociative chemisorption of methane on Ni(100), Ni(110), and Ni(111) is known from experiments (2, 3) to be almost the same, corresponding to an activation energy of ca. 52 kJ/mol. Thus from the value at 723 K,  $k_2$  can be calculated at the two other temperatures, 773 and 823 K, leaving only one parameter,  $k_3$ , to be adjusted in the comparison with the experimental values. The rates calculated using the  $k_2$  and  $k_3$  values shown in Table 2 are compared with the experimental rates in Figs. 4 and 5 for the values obtained at 773 and 823 K, respectively. The  $k_3$  values have been chosen to give good agreement at the lower rates, regardless of the higher ones in the fitting procedure. The reason is that both calculations and experiments with crushed pellets strongly indicate that the values measured for the higher rates are influenced by diffu-

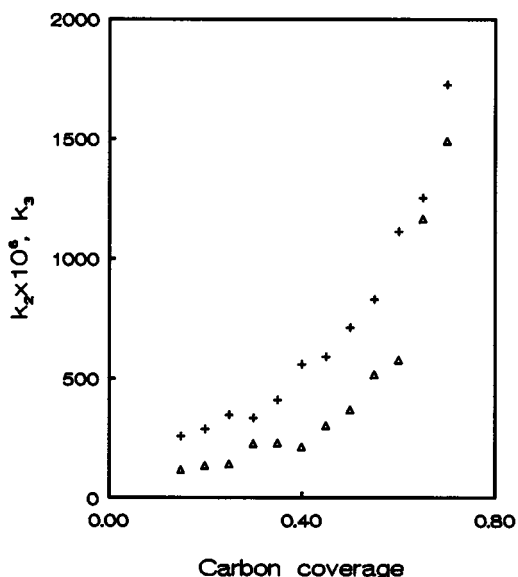


FIG. 3. Carbon coverage dependence of the rate constants  $k_2$  and  $k_3$  for the optimized model. (+)  $k_2 \times 10^6$ , ( $\Delta$ )  $k_3$ .

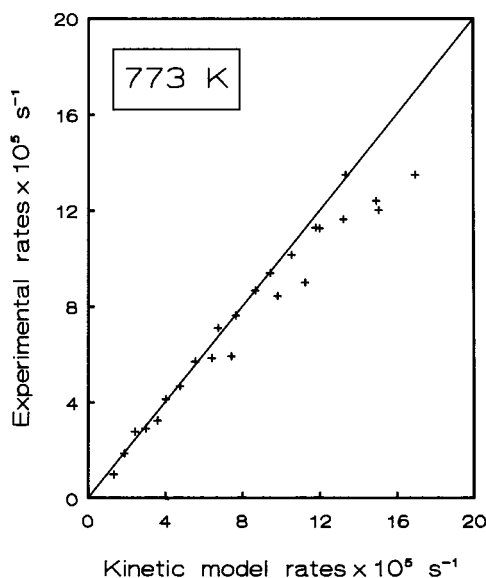


FIG. 4. Comparison between calculated and measured rates of carbon formation on Ni/SiO<sub>2</sub> at 773 K from CH<sub>4</sub> + H<sub>2</sub> gas mixtures. The rate unit is 10<sup>-5</sup> gcarbon/gcat/s.

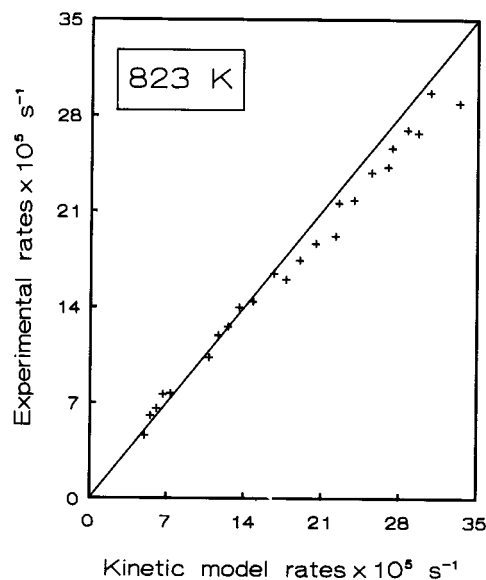


FIG. 5. Comparison between calculated and measured rates of carbon formation on Ni/SiO<sub>2</sub> at 823 K from CH<sub>4</sub> + H<sub>2</sub> gas mixtures. The rate unit is 10<sup>-5</sup> gcarbon/gcat/s.



sion restrictions (11). This assumption is also in accordance with the fact that the higher experimental rates are all deviating from the calculated ones toward smaller values.

Assuming that the temperature dependence of  $k_3$  can be described by an Arrhenius expression we estimate the activation energy of the forward rate of step 3 from the results at the three temperatures to be about 120 kJ/mol.

#### 6. CONCLUSIONS

A microkinetic model for carbon formation on nickel surfaces exposed to CH<sub>4</sub> + H<sub>2</sub> gas mixtures has been constructed. It gives good agreement with experimental rates for carbon formation on a Ni/SiO<sub>2</sub> catalyst. It shows that the reaction consists of the same sequence of steps on iron and nickel. However, while the reaction on iron can be described by assuming a rate-limiting step, viz. the dehydrogenation of the surface methyl, it is necessary also to treat the dissociative chemisorption of CH<sub>4</sub> as deviating from equilibrium on nickel under the present conditions. The model rates depend sensitively on the values used for the chemisorption bond energies of carbon and hydrogen. The values giving best agreement with the experiment are within the range of values expected from calculations and from other experiments.

#### ACKNOWLEDGMENTS

This work has been supported by the Danish Research Councils through the Center for Surface Reactivity. The visits of M. T. Tavares at the Haldor Topsøe Research Laboratories have been supported within the COMETT program.

#### REFERENCES

1. Lee, M. B., Yang, Q. Y., Tang, S. L., and Ceyer, S. T., *J. Chem. Phys.* **87**, 2724 (1987).
2. Beebe, T. P., Jr., Goodman, D. W., Kay, B. D., and Yates, J. T., Jr., *J. Chem. Phys.* **87**, 2305 (1987).
3. Chorkendorff, I., Alstrup, I., and Ullmann, S., *Surf. Sci.* **227**, 291 (1990).
4. Grabke, H. J., *Metall. Trans.* **1**, 2972 (1970).
5. Lázár, K., Kertész, K., Császár-Gilicze, É., and Konczos, G., *Z. Metallkd.* **71**, 124 (1980).
6. Figueiredo, J. L., and Trimm, D. L., *J. Catal.* **40**, 154 (1975).
7. Audier, M., and Coulon, M., *Carbon* **23**, 317 (1985).
8. Bernardo, C. A., Alstrup, I., and Rostrup-Nielsen, J. R., *J. Catal.* **96**, 517 (1985).
9. Baker, R. T. K., Harris, P. S., Thomas, R. B., and Waite, R. J., *J. Catal.* **30**, 86 (1973).
10. Rostrup-Nielsen, J. R., and Trimm, D. L., *J. Catal.* **48**, 155 (1977).
11. Tavares, M. T., and Alstrup, I., to be published.
12. Nørskov, J. K., and Stoltze, P., *Surf. Sci.* **189/190**, 91 (1987).
13. "JANAF Thermochemical Tables," 2nd ed., NSRDS-NBS 37, 1971.
14. Andersson, S., in "Proceedings, 7th International Vac. Congr.; Proceedings, 3rd Int. Conf. Solid Surfaces," Vienna, p. 1019, 1977.
15. Christmann, K., *Z. Naturforsch. A.* **34**, 22 (1979).
16. Siegbahn, P. E. M., and Wahlgren, U., "Cluster Modelling of Chemisorption Energetics," in press.
17. Siegbahn, P. E. M., and Panas, I., *Surf. Sci.* **240**, 37 (1990).
18. Lehwald, S., unpublished. Results quoted in Ibach, H., and Mills, D. L., "Electron Energy Loss Spectroscopy and Surface Vibrations," Table 6.1, p. 277. Academic Press, San Diego, 1982.
19. Isett, L. C., and Blakely, J. M., *Surf. Sci.* **58**, 397 (1976).
20. Takeuchi, A., and Wise, H., *J. Phys. Chem.* **87**, 5372 (1983).
21. Berndt, R., Toennies, J. P., and Wöll, Ch., *J. Electron. Spectrosc.* **44**, 183 (1987).
22. Sørensen, O., Tavares, M. T., and Alstrup, I., to be published.
23. Schouten, F. C., Gijzeman, O. L. J., and Bootsma, G. A., *Surf. Sci.* **87**, 1 (1979).
24. Ko, E. I., and Madix, R. J., *Appl. Surf. Sci.* **3**, 236 (1979).